Available online at www.sciencedirect.com

ScienceDirect

Mendeleev Commun., 2021, **31**, 385–387

Mendeleev Communications

Influence of hydrothermal conditions on the phase transformations of amorphous alumina

Aliya N. Mukhamed'yarova,* Svetlana R. Egorova, Oksana V. Nosova and Alexander A. Lamberov

A. M. Butlerov Institute of Chemistry, Kazan Federal University, 420008 Kazan, Russian Federation.
E-mail: anm03@list.ru

DOI: 10.1016/j.mencom.2021.05.034

Amorphous Al_2O_3 transforms into the pseudoboehmite and boehmite phases of AlO(OH) under hydrothermal conditions. Specific surface area, pore volume and the amount of acidic sites decrease upon complete conversion of amorphous Al_2O_3 into boehmite.

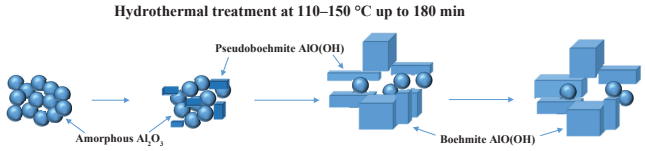

Keywords: amorphous alumina, hydrothermal treatment, alumina catalyst, porous system, amount of acidic sites.

γ-Alumina is widely used in chemical industry as a catalyst, a carrier and a sorbent.[1–4] It is generally produced by heat treatment of its AlO(OH) precursors, including pseudoboehmite (Pbm) and boehmite (Bm), which in turn can be synthesized by hydrolysis of aluminum alkoxides with a possibility to effectively adjust the phase composition and properties of intermediate aluminum hydroxides.[5,6] The hydrolysis includes conversion of OR groups into the OH ones and represents a stepwise process with the lowest rate in its last stage.[7] The conversion rate depends on the nature of the OR groups, the temperature as well as the volume of water in the reaction zone. The products of the aluminum alkoxides hydrolysis are aluminoxane stabilized in the structure of Bm as well as amorphous aluminum hydroxide.[8–11] After subsequent heat treatment up to 550 °C the aluminoxane–Bm mixture transforms into γ-Al_2O_3, while the hydroxide turns into amorphous Al_2O_3.[12,13]

Investigation of amorphous Al_2O_3 is typically hampered by its disordered structure,[8–13] in contrast to the crystalline γ-Al_2O_3 one. This phase difference represents the main reason for the decline of conversion and selectivity of alumina catalysts employed in vapor-phase dehydration of alcohols or isomerization of olefins, which makes relevant a search for effective synthetic routes to monophasic Al_2O_3. Hydrothermal treatment is one of the approaches to accomplish the hydrolysis of amorphous aluminum compounds to its crystalline monohydroxide. It is known[14] that the amorphous component crystallizes into Bm during the hydrothermal reaction, and this allows one to adjust the properties of alumina catalyst for further use in the skeletal isomerization of *n*-butenes. In our research,[15] the hydrolysis product of aluminum isopropoxide was converted to an oxide form to lower the impact of polyaluminoxane on the phase transformation of the obtained amorphous Al_2O_3 and on the properties of products of its further low-temperature hydrothermal conversion. In this work, we investigated the related phase transformations, the porous system of the products obtained by hydrothermal treatment of amorphous Al_2O_3 under different conditions as well as acidic properties of alumina synthesized by heat treatment of aluminum hydroxides.

The starting amorphous Al_2O_3 was obtained by hydrolysis of aluminum isopropoxide with water vapor and subsequent heating at 550 °C for 2 h.[15] Its following hydrothermal treatment in aqueous suspension at 110–150 °C with the water vapor pressure of 0.14–0.48 MPa for up to 180 min resulted in general in a mixture of Pbm, Bm and bayerite (Brt) (Figure 1, Figures S1 and S2, see Online Supplementary Materials),† the last form was detected in less than 8 wt% only at lower temperatures at the beginning of the treatment and further transformed into Pbm.

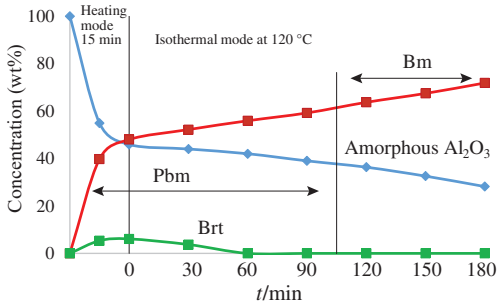

Figure 1 Hydrothermal conversion of amorphous Al_2O_3 into Pbm, Bm and Brt at 120 °C.

† Phase composition was determined by X-ray diffraction (XRD) using a MiniFlex 600 instrument (Rigaku) with a D/teX Ultra detector and CuKα long-wave radiation (40 kW, 15 mA). The composition of samples was measured by combined thermogravimetry and differential scanning calorimetry (TG–DSC) using an STA 449 C Jupiter thermo-microbalance (Netzsch) at 30–1000 °C with heating rate of 10 °C min^{-1} in Ar stream as well as by mass spectrometry after heating in a He flow using a ThermoStar GSD 320 T gas analyzer (Pfeiffer Vacuum).

Particle morphology was explored by SEM using a Merlin autoemission high-resolution microscope (Carl Zeiss) as well as by TEM using an HT7700 instrument (Hitachi).

Porous system was investigated by low-temperature nitrogen adsorption using an ASAP 2460 surface area and porosity analyzer (Micromeritics).

Surface acidity was analyzed by temperature-programmed desorption of ammonia using a flow-type device equipped with a ChemBET Pulsar thermal conductivity detector (Quantachrome Instruments) after the samples treatment in a muffle furnace at 550 °C for 3 h with a heating rate of 5 °C min^{-1}.

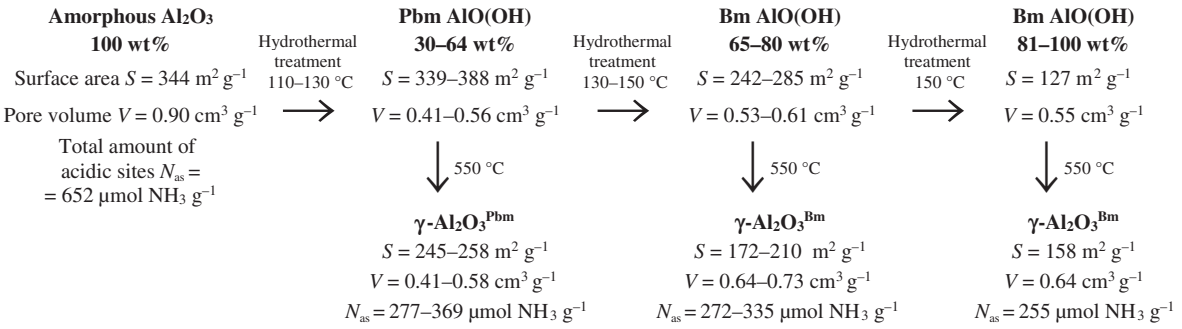

Scheme 1

Maximum fraction of Pbm (63.9 wt%) was found at 130 °C after 60 min, while after 90 min at constant temperature in the range of 110–130 °C it crystallized into Bm.

The transformation of amorphous alumina into Pbm and Bm under hydrothermal conditions proceeds through the dissolution–precipitation mechanism.[16,17] Spherical Al_2O_3 particles of ~11 nm diameter constitute large aggregates of 3–133 μm size[15] and initially crystallize in the needle- and plate-like Pbm particles with ~20 nm width and 70–100 nm length. Then these needles/plates grow into parallelepiped-like Bm particles with 27–45 nm width and 73–155 nm length composed of rhombic plates (Figure S3). The influence of these phase and morphologic transformations on the porous system of the hydrothermal treatment products was explored in detail (Figures S4–S8). It is known that starting amorphous alumina contributes to the pore volume and specific surface area of the products with its pore volume of 0.90 cm^3 g^{-1} caused by the mesopores with a shoulder on the differential curve of their volume distribution at ~10 nm and the micropores formed between the coarse agglomerates of the spherical particles, as well as with its specific surface area of 344 m^2 g^{-1} due to ~60% of mesopores with 3–5 nm diameter.[15] Pbm contributes new thin mesopores with maxima in the differential curve of their diameter distribution at 2.8 and 3.8 nm. This in turn leads to an increase in the specific surface area of the hydrothermal products to 388 m^2 g^{-1} and the decrease in their pore volume to 0.41 cm^3 g^{-1}. Bm does not actually contain thin pores, the pore diameter is 21 nm and the corresponding specific surface area is as low as 127 m^2 g^{-1}.

The hydrothermal treatment products were further transformed into amorphous and/or crystalline Al_2O_3 after heat treatment at 550 °C. Alumina obtained from Pbm (γ-$Al_2O_3^{Pbm}$) inherited thin pores with diameter of 3.8 nm from its precursor, while the specific surface area and pore volume decreased to 248 m^2 g^{-1} and 0.51 cm^3 g^{-1}, respectively, with lowering to 30 wt% the content of amorphous Al_2O_3 in the hydrothermal product. Specific surface area value was stabilized (245–258 m^2 g^{-1}) with an increase in the γ-$Al_2O_3^{Pbm}$ part in the product to ~60 wt% . Pore volume elevated to 0.41–0.58 cm^3 g^{-1} due to the growth of pore diameter to 7.0–14.3 nm. With appearance of γ-$Al_2O_3^{Bm}$ in the composition of alumina with 40 wt% of amorphous Al_2O_3 after the hydrothermal treatment, the pore volume increased to 0.64 cm^3 g^{-1} while the surface area diminished to 172 m^2 g^{-1}.

Acidic properties of the alumina mixture are in general determined by superposition of the individual phases acidity. Starting amorphous Al_2O_3 is characterized by the highest acidity of 652 μmol NH_3 g^{-1} due to its maximal surface area, with medium acidic sites predominating (46%). After transformation of its 30 wt% into γ-$Al_2O_3^{Pbm}$, the total amount of acidic sites decreased to 326 μmol NH_3 g^{-1}, *i.e.*, by two times. The amount of acidic sites in the alumina mixture was stabilized at 277–369 μmol NH_3 g^{-1} with growth of the γ-$Al_2O_3^{Pbm}$ content up to 60 wt%, and the amount of weak acid sites increased from 151 to 195 μmol NH_3 g^{-1}. The similar pattern revealed after γ-$Al_2O_3^{Bm}$ had appeared in the alumina mixture, with total amount of acidic sites 255 μmol NH_3 g^{-1} for the samples with more than 80 wt% γ-$Al_2O_3^{Bm}$, mainly due to the decrease in the weak acidic sites amount from 208 to 96 μmol NH_3 g^{-1}.

The changes in phase composition, texture characteristics and acidic properties originated from the transformations of amorphous alumina under hydrothermal conditions are collected in Scheme 1.

Thus, as a result of hydrothermal treatment of amorphous alumina at 110–150 °C with pressurised saturated water vapor for up to 3 h, Pbm, Bm and Bt (up to 8.0 wt%), were formed. The transformation of 64 wt% of amorphous Al_2O_3 into Pbm was accompanied by a slight increase in the specific surface area from 344 to 388 m^2 g^{-1} and a decrease in the total pore volume from 0.90 to 0.41 cm^3 g^{-1} due to formation of thin pores with diameters 2.8–3.8 nm between the primary particles of Pbm. Further crystallization to ~80 wt% of Bm caused an increase in the pore volume to 0.53–0.61 cm^3 g^{-1} originated mainly from an elevation of the volume of pores with diameter more than 5 nm. After heat treatment at 550 °C for 3 h, the products of hydrothermal treatment of Pbm and Bm conversed completely into γ-$Al_2O_3^{Pbm}$ and γ-$Al_2O_3^{Bm}$, respectively, while amorphous Al_2O_3 was stable up to ~700 °C. γ-$Al_2O_3^{Pbm}$ inherited the fine-pore system of Pbm, which led to a decrease in the specific surface area from 344 to 245–258 m^2 g^{-1} and the pore volume from 0.90 to 0.41–0.58 cm^3 g^{-1}. The porous system of aluminum oxides obtained from Bm is characterized by enlarged pore of diameter of more than 10 nm, which leads to an increase in the total pore volume to 0.64 cm^3 g^{-1} and a decrease in surface area to 158 m^2 g^{-1}. The total number of acidic sites on the surface of aluminum oxides correlates well with the specific surface area. Amorphous Al_2O_3 is characterized by predominance (47%) of medium-strength acidic sites with the energy of ammonia desorption E_d = 110–142 kJ mol^{-1}. γ-$Al_2O_3^{Pbm}$ and γ-$Al_2O_3^{Bm}$ have weak acidic sites with E_d less than 110 kJ mol^{-1}. As a result of the hydrothermal treatment and the subsequent maintenance at 550 °C, the total amount of acidic sites reduced from 652 for amorphous Al_2O_3 to 255 μmol NH_3 g^{-1} for γ-$Al_2O_3^{Bm}$. The results obtained allows one to expect the stable operation of a catalyst obtained by hydrothermal treatment of amorphous alumina in, for example, dehydration of 1-phenylethanol into styrene, due to a sufficient number of the surface acidic sites and a pore size of more than 10 nm.

Online Supplementary Materials

Supplementary data associated with this article can be found in the online version at doi: 10.1016/j.mencom.2021.05.034.

References

1 N. S. Smirnova, P. V. Markov, G. N. Baeva, A. V. Rassolov, I. S. Mashkovsky, A. V. Bukhtiyarov, I. P. Prosvirin, M. A. Panafidin, Ya. V. Zubavichus, V. I. Bukhtiyarov and A. Yu. Stakheev, *Mendeleev Commun.*, 2019, **29**, 547.

2 A. A. Shesterkina, L. M. Kozlova, I. V. Mishin, O. P. Tkachenko, G. I. Kapustin, V. P. Zakharov, M. S. Vlaskin, A. Z. Zhuk, O. A. Kirichenko and L. M. Kustov, *Mendeleev Commun.*, 2019, **29**, 339.

3 P. V. Markov, N. S. Smirnova, G. N. Baeva, A. V. Bukhtiyarov, I. S. Mashkovsky and A. Yu. Stakheev, *Mendeleev Commun.*, 2020, **30**, 468.

4 V. I. Bogdan, A. E. Koklin, A. N. Kalenchuk and L. M. Kustov, *Mendeleev Commun.*, 2020, **30**, 462.

5 E. V. Petrova, A. F. Dresvyannikov and A. I. Khairullina, *Russ. Chem. Bull., Int. Ed.*, 2020, **69**, 926 (*Izv. Akad. Nauk, Ser. Khim.*, 2020, 926).

6 R. Marinkoviae-Neduein, E. Kis, M. Duriae, G. Boskoviae, J. Kiurski and R. Miatiae, *Stud. Surf. Sci. Catal.*, 1998, **113**, 399.

7 V. A. Dzis'ko, A. P. Karnaukhov and D. V. Tarasova, *Fiziko-khimicheskiye osnovy sinteza okisnykh katalizatorov (Physico-Chemical Principles of the Synthesis of Oxide Catalysts)*, Nauka, Novosibirsk, 1978 (in Russian).

8 V. A. Dzisko, A. S. Ivanova and G. P. Vishniakova, *Kinet. Catal.*, 1976, **17**, 415 (*Kinet. Katal.*, 1976, **17**, 483).

9 X. Cheng, Y. Liu and D. Chen, *J. Phys. Chem. A*, 2011, **115**, 4719.

10 I. A. Yamanovskaya, T. V. Kusova, A. S. Kraev, A. V. Agafonov, G. A. Seisenbaeva and V. G. Kessler, *J. Sol–Gel Sci. Technol.*, 2019, **92**, 293.

11 B. Huang, C. H. Bartholomew and B. F. Woodfield, *Microporous Mesoporous Mater.*, 2014, **183**, 37.

12 G. Brieger, S. W. Watson, D. G. Barar and A. L. Shene, *J. Org. Chem.*, 1979, **44**, 1340.

13 N. K. Sahu, C. K. Sarangi, B. Dash, B. C. Tripathy, B. K. Satpathy, D. Meyrick and I. N. Bhattacharya, *Trans. Nonferrous Met. Soc. China*, 2015, **25**, 615.

14 I. N. Mukhambetov, S. R. Egorova, A. N. Mukhamed'yarova and A. A. Lamberov, *Appl. Catal., A*, 2018, **554**, 64.

15 A. N. Mukhamed'yarova, O. V. Nesterova, K. S. Boretsky, J. D. Skibina, A. V. Boretskaya, S. R. Egorova and A. A. Lamberov, *Coatings*, 2019, **9**, 41.

16 C. Kaya, J. Y. He, X. Gu and E. G. Butler, *Microporous Mesoporous Mater.*, 2002, **54**, 37.

17 F. Karouia, M. Boualleg, M. Digne and P. Alphonse, *Adv. Powder Technol.*, 2016, **27**, 1814.

Received: 15th February 2021; Com. 21/6452